

# Mean-field theory for pedestrian outflow through an exit

Daichi Yanagisawa and Katsuhiro Nishinari

*Department of Aeronautics and Astronautics, School of Engineering, The University of Tokyo, Hongo, Bunkyo-ku, Tokyo 113-8656, Japan*  
 (Received 26 August 2007; published 19 December 2007)

The average pedestrian flow through an exit is one of the most important indices in evaluating pedestrian dynamics. In order to study the flow in detail, the floor field model, which is a crowd model using cellular automata, is extended by taking into account realistic behavior of pedestrians around the exit. The model is studied by both numerical simulations and cluster analysis to obtain a theoretical expression for the average pedestrian flow through the exit. It is found quantitatively that the effects of exit door width, the wall, and the pedestrian mood of competition or cooperation significantly influence the average flow. The results show that there is a suitable width and position of the exit according to the pedestrians' mood.

DOI: 10.1103/PhysRevE.76.061117

PACS number(s): 02.50.-r, 02.70.Uu, 34.10.+x, 45.70.Vn

## I. INTRODUCTION

Pedestrian dynamics has received growing interest from physicists over recent decades, since it shows new collective behaviors such as dynamical phase transitions and spontaneous symmetry breaking [1–4]. Helbing *et al.* designed the social force model [2], which reproduces typical pedestrian behavior such as arching, lane formation, and oscillations of direction at bottlenecks. It is based on a system of coupled differential equations which have to be solved by using, e.g., a molecular dynamics approach as in the study of granular matter. Another approach is discrete modeling using cellular automata, which has been actively studied in recent years [4–8]. In this paper, we study the floor field (FF) model, which is a cellular automaton model, introducing two kinds of FFs, i.e., the static (SFF) and the dynamic FF (DFF) [9], to move pedestrians from one cell to another. The two FFs, which are explained in Sec. II, enable us to simulate egress processes from complex rooms of arbitrary geometry quite efficiently. Kirchner *et al.* discovered that the pedestrian mood of competition or cooperation increases or decreases the evacuation time [10]. Moreover, an obstacle in front of the exit will shorten the evacuation time in some cases in the simulation of egress processes [11]. Many extended models have been proposed up to now to make the FF model more realistic. For example, the strength of the inertia of pedestrians, which suppresses quick changes of the direction of motion, is considered in [12]. Henein *et al.* have taken into account physical forces between pedestrians by adding a dynamic force field to the FF model [13].

Most of these studies are based on simulations, and there are few analytical results because of the complexity of the rules of motion and the two-dimensionality. In this paper, we present an analytical result for outflow through an exit, which is one of the most important indices in evaluating evacuation dynamics. Kirchner *et al.* obtained an expression for the average number of evacuated persons  $\langle N \rangle$  from an exit with one cell's width as a function of the time step and the friction parameter  $\mu$  using the mean-field approximation [11]. Here we introduce the bottleneck parameter  $\beta$ , which makes pedestrian behaviors around the exit more realistic. We have succeeded in calculating the average flow  $\langle Q \rangle$  as a function of  $\beta$ ,  $\mu$ , and the width of the exit door,  $w$ , by the

cluster approximation. As far as we know, the analytical expression for the average flow through an exit with arbitrary width is derived for the first time in this paper.

This paper is organized as follows. In Sec. II we briefly review the FF model and introduce the parameter  $\beta$  in Sec. III. We calculate the average flow  $\langle Q \rangle$  by the cluster approximation in Sec. IV, and  $\langle Q \rangle$  obtained from simulation and the theoretical expression are compared in Sec. V. In Secs. VI and VII we consider how the mood of the pedestrians and a wall beside the exit influence the average flow. Both effects are explained using the contour plots of the average flow in Sec. VIII. Section IX is devoted to summary and discussion.

## II. FLOOR FIELD MODEL

### A. Floor field

We consider a situation where every pedestrian in a room moves to the same exit. The room is divided into cells as given in Fig. 1. The person-shaped silhouettes represent pedestrians; the letters **E** and **O** represent the exit cell and obstacle cells, respectively. Each cell contains only a single pedestrian at most. At every time step, pedestrians choose which cell to move from five cells: the cell in which the pedestrian stands now [ $(i,j)=(0,0)$ ] and the Neumann neighboring cells [ $(i,j)=(0,1), (0,-1), (1,0), (-1,0)$ ] (Fig. 2). Two kinds of FF determine the probability of movement direction. The SFF  $S_{ij}$ , which is the shortest distance to the exit cell, is given by the  $L^2$  norm as

$$S_{ij} = \sqrt{|x_{ij} - x_{\text{exit}}|^2 + |y_{ij} - y_{\text{exit}}|^2}, \quad (1)$$

where  $(x_{ij}, y_{ij})$  and  $(x_{\text{exit}}, y_{\text{exit}})$  are the coordinates of the cell  $(i, j)$  and the exit cell, respectively. However, when there is

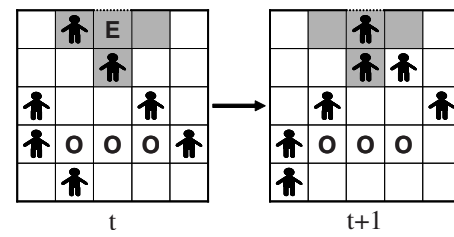


FIG. 1. Schematic view of an evacuation simulation by the FF model. Pedestrians proceed to the exit by one cell at most for each time step.

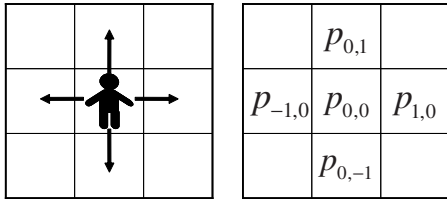


FIG. 2. Target cells for a pedestrian at the next time step. The motion is restricted to the Neumann neighborhood in this model.

an obstacle on the way to the exit, the SFF is calculated by making a detour around it (Fig. 3). Thus, the SFF is not simply described by (1) in that case [12]. Pedestrians move to a cell that has a smaller SFF than the cell they occupy and hence go to the exit. The DFF  $D_{ij}$  at cell  $(i,j)$  is the number of footprints left by the pedestrians. Pedestrians interact with each other using footprints as do ants using their pheromones. The long-ranged interaction through the pedestrians' sight is approximated by a short-ranged interaction around the pedestrians by using the DFF. This shortens the calculation time dramatically. When pedestrians move to the common exit, it is known in reality that they tend to follow each other. This phenomenon can be reproduced by moving pedestrians to a cell with a bigger DFF (Fig. 4). The DFF has its own dynamics, namely, diffusion and decay, which leads to broadening, dilution, and finally vanishing of the footprints [12].

Therefore, in this model, the transition probability  $p_{ij}$  for a move to a neighbor cell  $(i,j)$  is determined by the following expression:

$$p_{ij} = N \xi_{ij} \exp(-k_s S_{ij} + k_d D_{ij}). \quad (2)$$

Here the values of the FFs  $S_{ij}$  and  $D_{ij}$  at each cell  $(i,j)$  are weighted by two sensitivity parameters  $k_s$  and  $k_d$  with the normalization  $N$ . There is a minus sign before  $k_s$  since the pedestrian moves to a cell with a lower SFF.  $\xi_{ij}$  returns to 0 for an obstacle or a wall cell and returns to 1 for other kinds of cells. Note that in our paper a cell occupied by a pedestrian is not regarded as an obstacle cell; thus it affects the normalization  $N$ .

## B. Conflict resolution and friction

Due to the use of parallel dynamics, it can happen that two or more pedestrians choose the same target cell in the

$S = 2$	1	E	0	1	2
$\sqrt{5}$	$\sqrt{2}$	1	$\sqrt{2}$	$\sqrt{5}$	
$2\sqrt{2}$	$\sqrt{5}$	2	$\sqrt{5}$	$2\sqrt{2}$	
$2\sqrt{2}+1$	O	O	O	$2\sqrt{2}+1$	
$2\sqrt{2}+2$	$2\sqrt{2}+3$	$2\sqrt{2}+4$	$2\sqrt{2}+3$	$2\sqrt{2}+2$	

FIG. 3. Static floor field constructed by the exit E. The numbers in each cell represent the Euclidean distances from the exit cell.

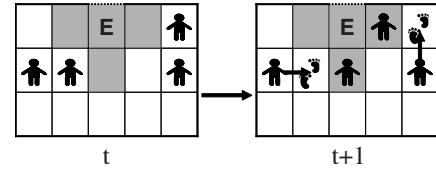


FIG. 4. Schematic view of dynamic floor field. At  $t+1$  two pedestrians who could move leave footprints at the cells they occupied at  $t$ . Remaining pedestrians are likely to move to cells containing footprints.

update procedure. Such situations are called conflicts in this paper. To describe the dynamics of a conflict in a quantitative way, the friction parameter  $\mu \in [0, 1]$  was introduced in Refs. [10,11]. This parameter describes clogging and sticking effects between the pedestrians. In a conflict, the movement of all involved pedestrians is denied with probability  $\mu$ , i.e., all pedestrians remain in their cells. Therefore, the conflict is resolved with probability  $1-\mu$ , and one of the pedestrians is allowed to move to the desired cell (Fig. 5). The pedestrian that actually moves is then chosen randomly with equal probability. In a situation with large  $\mu$ , pedestrians are competitive and do not give way to others. Thus they hardly move due to the conflict between them. In contrast, in a situation with small  $\mu$ , they give way and cooperate each other.

## C. Update rules

The FF model consists of the following five steps per unit time step, and is repeated until all pedestrians have exited or the maximum number of calculation time steps have passed.

- (1) Calculate each pedestrian's transition probability by (2) and the values of the SFF and DFF.
- (2) Move pedestrians based on the calculated transition probability. If there are cells which are possibly occupied by more than two pedestrians, solve conflicts by the means of Sec. II B.
- (3) Diffuse and decay the DFF of every cell.
- (4) Pedestrians who could move at step 2 increase the value of the DFF by 1 at the cell they occupy.
- (5) Pedestrians who stand on exit cells are removed from the room.

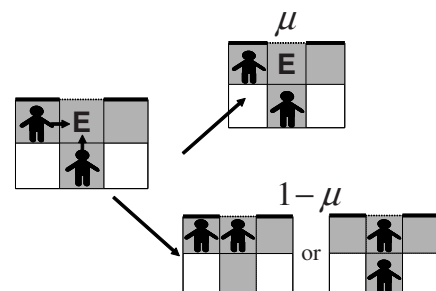


FIG. 5. Method of solving conflicts. In a conflict situation, all involved pedestrians remain at their cells with probability  $\mu$ . One of them is randomly allowed to move to the desired cell with probability  $1-\mu$ .

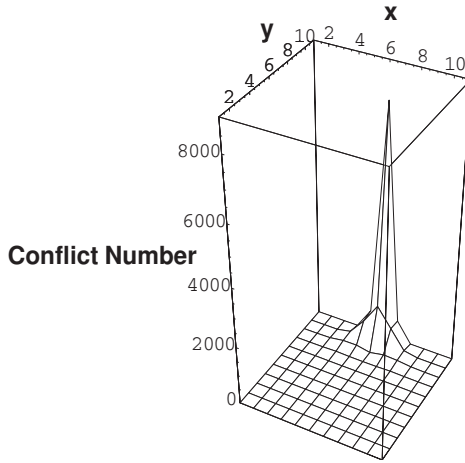


FIG. 6. Number of conflicts in a competitive situation. We simulated in a room of  $11 \times 11$  cells with one cell exit for 11 000 time steps and accumulated the value for 1001–11 000 time steps. The cell at (6,10) is the exit cell. We find that more than 60% of conflicts occur at the exit cell, and the probability of conflict there is about 80%.

In the following, we consider only the effect of the SFF and ignore the DFF for simplicity. Thus the steps 3 and 4 are not considered in this paper. The DFF plays a role in mimicking the long-ranged interaction among pedestrians by a short-ranged one. Therefore, ignoring the DFF is justified when we consider pedestrian behaviors only near an exit as we do here. We also confirm that results in this paper are not significantly changed by the introduction of the DFF.

### III. INTRODUCTION OF AN ADDITIONAL PARAMETER NEAR THE EXIT

In real situations, pedestrian density depends on the area in the room. While there are few pedestrians near a corner, there are many pedestrians gathering around the exit. Therefore, pedestrians often conflict with each other around the exit, and an arc of pedestrians is likely to be formed in front of the exit due to friction between them [2]. Figure 6 shows the number of conflicts in an egress process in a competitive situation in 10 000 time steps. The exit is set at  $(x,y)=(6,10)$  in the figure. We see 7842 conflicts at the exit cell, about 1000 at the five Moore neighbor cells of the exit, and fewer than 110 at other cells. This result says that more than 60% of conflicts occur at the exit cell, and the probability of conflict there is about 80%. Since pedestrians know this fact by experience, they walk fast when they are far from the exit, while they walk slowly or give way to each other around the exit. That is to say, the walking velocity depends on the area in the room. In the usual FF model, however, the transition probability, i.e., the walking velocity, is the same wherever the pedestrians are. To take into account this situation, we introduced a parameter  $\beta \in [0, 1]$  which we call the bottleneck parameter. The transition probability of pedestrians who occupy one of the Neumann neighboring cells of the exit cell is described as follows:

$$p_{ij} = \beta \bar{N} \xi_{ij} \exp(-k_s S_{ij} + k_d D_{ij}) \quad [(i,j) \neq (0,0)],$$

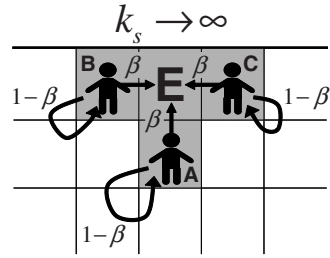


FIG. 7. Approximation of the transition probabilities at Neumann neighboring cells of the exit when the width of the exit  $w=1$ . When  $k_s$  is large,  $p_{0,1} \rightarrow \beta$ ,  $p_{0,0} \rightarrow 1-\beta$ , and  $p_{0,-1}, p_{1,0}, p_{-1,0} \rightarrow 0$  for a pedestrian A. Similarly,  $p_{1,0} \rightarrow \beta$  for a pedestrian B and  $p_{-1,0} \rightarrow \beta$  for a pedestrian C.

$$p_{0,0} = (1 - \beta) + \beta \bar{N} \exp(-k_s S_{0,0} + k_d D_{0,0}), \quad (3)$$

where  $\bar{N}$  is represented as

$$\bar{N} = \left( \sum_{i,j} \xi_{ij} \exp(-k_s S_{ij} + k_d D_{ij}) \right)^{-1}. \quad (4)$$

The transition probability of other cells is the same as (2). Here, if  $\beta=0$ ,  $p_{ij}=0$  [ $(i,j) \neq (0,0)$ ] and  $p_{0,0}=1$ , which means that nobody moves to the exit cell; while, if  $\beta=1$ , the transition probability is the same as (2), which means that pedestrians move fast as they are far from the exit.  $\beta$  controls the velocity of the pedestrians who are at the neighboring cells of the exit. In Ref. [11], the parameter  $k_s$  is used to describe the velocity of the pedestrians. However, since a small value of  $k_s$  means lack of knowledge of the exit position, pedestrians sometimes move backward. In reality, pedestrians move to the exit along the shortest path and slow down near the exit to avoid conflicts with others. Therefore,  $\beta$  is not compensated by  $k_s$ , and we expect that more realistic pedestrian behavior is described by the parameter  $\beta$ . When  $k_s$  is large, the transition probabilities of pedestrians at neighboring cells of the exit are approximated as in Fig. 7. This simplification enables us to analyze the pedestrian behavior theoretically.

### IV. ANALYTICAL EXPRESSION FOR THE AVERAGE FLOW USING THE CLUSTER APPROXIMATION

In the FF model with added  $\beta$ , when  $k_s$  is large, it is almost sure that pedestrians move to the exit cells with probability 1 if they are far from the exit and with probability  $\beta$  in the Neumann neighboring cells of the exit. Therefore, in this section we focus on the exit cells and their neighbor cells and calculate an analytical expression for the average pedestrian flow through the exit by the cluster approximation. The flow is defined as the number of evacuated persons per one time step through an exit. We suppose that a big jam is formed around the exit. This enables us to simplify the situation such that only the SFF affects the pedestrians' motion.

First, we calculate the flow when the width of the exit  $w=1$ . The transition probabilities are defined in Fig. 8. We consider two kinds of states of a cell, 1 and 0, which represent that a pedestrian exists at the cell or not. Therefore, in the case  $w=1$ , there are 16 different states for these four cells

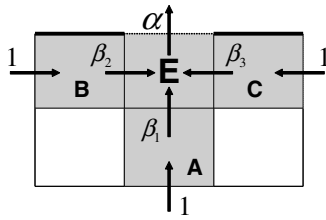


FIG. 8. Cluster approximation at the exit with one cell. 1,  $\alpha$ ,  $\beta_1$ ,  $\beta_2$ , and  $\beta_3$  represent transition probabilities.

in total. Since we assume that a big jam exists at the exit, pedestrians enter into three neighboring cells of the exit with the probability 1.  $\alpha$  is the probability of getting out from the exit cell, which is set as 1 throughout this paper. We define  $p_t(0)$  as the probability that a pedestrian is not at the exit cell at time step  $t$  and  $p_t(1)$  as the probability that a pedestrian is at the exit cell at time step  $t$ . The master equations are described as follows:

$$\begin{bmatrix} p_{t+1}(0) \\ p_{t+1}(1) \end{bmatrix} = \begin{bmatrix} 1 - r & \alpha \\ r & 1 - \alpha \end{bmatrix} \begin{bmatrix} p_t(0) \\ p_t(1) \end{bmatrix}. \quad (5)$$

Here  $r$  represents the probability that a pedestrian enters into the exit cell from the three Neumann neighboring cells, which is described as follows:

$$\begin{aligned} r = & \beta_1(1 - \beta_2)(1 - \beta_3) + \beta_2(1 - \beta_3)(1 - \beta_1) \\ & + \beta_3(1 - \beta_1)(1 - \beta_2) + (1 - \mu)[\beta_1\beta_2(1 - \beta_3) \\ & + \beta_2\beta_3(1 - \beta_1) + \beta_3\beta_1(1 - \beta_2) + \beta_1\beta_2\beta_3]. \end{aligned} \quad (6)$$

The first term is the probability of a pedestrian coming from the cell A (Fig. 8). Similarly, the second and the third terms are the probabilities of a pedestrian coming from the cells B and C, respectively. The first three terms enclosed in square brackets in the fourth term represent the probability that one of the pedestrians enters into the exit cell from two of the three cells (A, B, and C) by resolving the conflicts. The last term enclosed in the square brackets represents a similar situation, but pedestrians enter into the exit cell from all three neighboring cells. By using (5) and (6) with the normalization condition

$$p_t(0) + p_t(1) = 1, \quad (7)$$

we obtain the stationary solution

$$p_\infty(1) = 1 - \frac{\alpha}{\alpha - a_2 - a_1 - a_0 - \mu(a_1 + 2a_0)}, \quad (8)$$

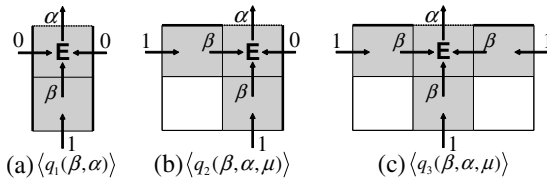


FIG. 9. Three special cases of Fig. 8. The arrow with transition probability 0 is interpreted as the existence of a wall that blocks pedestrian motion.

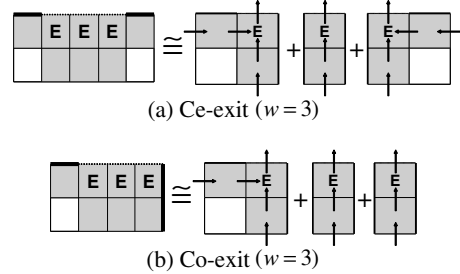


FIG. 10. Dividing an exit with three cells into three exits with one cell. The outflow also represents the sum of each flow.

$$\begin{aligned} a_0 &= -\beta_1\beta_2\beta_3, \\ a_1 &= \beta_1\beta_2 + \beta_2\beta_3 + \beta_3\beta_1, \\ a_2 &= -(\beta_1 + \beta_2 + \beta_3). \end{aligned} \quad (9)$$

Thus the number of pedestrians who can evacuate from an exit with one cell's width per one time step, i.e., the average pedestrian flow through the exit, is described as follows:

$$\begin{aligned} \langle Q(\beta_1, \beta_2, \beta_3, \alpha, \mu) \rangle &= \alpha p_\infty(1) \\ &= \alpha \left( 1 - \frac{\alpha}{\alpha - a_2 - a_1 - a_0 - \mu(a_1 + 2a_0)} \right). \end{aligned} \quad (10)$$

The expression for the average flow in the case  $\alpha = \beta_1 = \beta_2 = \beta_3 = 1$  was obtained in Ref. [11] as

$$\langle Q \rangle = \frac{1 - \mu}{2 - \mu}, \quad (11)$$

which can be recovered using  $\langle Q(1, 1, 1, 1, \mu) \rangle$ . Thus (10) is a generalization of the previous result (11).

Next we specify (10) by substituting 0 and  $\beta$  for  $\beta_1$ ,  $\beta_2$ , and  $\beta_3$  as follows:

$$\begin{aligned} (a) \quad \langle q_1(\beta, \alpha) \rangle &\equiv \langle Q(\beta, 0, 0, \alpha, \mu) \rangle = \frac{\alpha\beta}{\alpha + \beta}, \\ (b) \quad \langle q_2(\beta, \alpha, \mu) \rangle &\equiv \langle Q(\beta, \beta, 0, \alpha, \mu) \rangle \\ &= \alpha \left( 1 - \frac{\alpha}{\alpha + 2\beta - (1 + \mu)\beta^2} \right), \end{aligned}$$

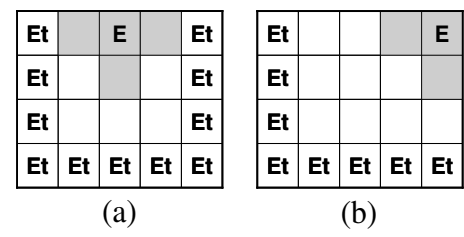


FIG. 11. 5x5-cell rooms with a one-cell exit. (a) Ce exit. (b) Co exit. E represents an exit cell, and Et represents an entrance cell where pedestrians come with probability 1.

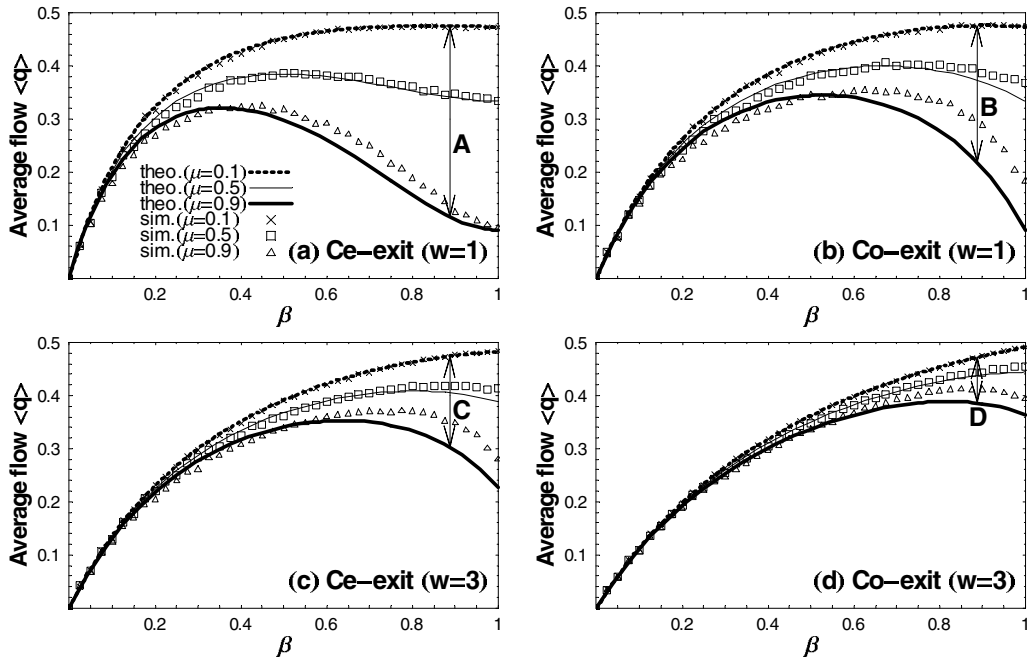


FIG. 12. Average flow  $\langle q \rangle$  as a function of  $\beta$  for different  $\mu$ , exit width  $w$ , and exit location. (a) Ce exit,  $w=1$ . (b) Co exit,  $w=1$ . (c) Ce exit,  $w=3$ . (d) Co exit,  $w=3$ . For  $\mu=0.9$  we clearly see a maximum of flow at an optimal  $\beta$ . The lengths of the arrows A, B, C, and D represent the differences between the flows for different  $\mu$ .

$$(c) \langle q_3(\beta, \alpha, \mu) \rangle \equiv \langle Q(\beta, \beta, \beta, \alpha, \mu) \rangle \\ = \alpha \left( 1 - \frac{\alpha}{\alpha + 3\beta - 3(1+\mu)\beta^2 + (1+2\mu)\beta^3} \right). \quad (12)$$

These expressions describe average flows through an exit with the configurations described in Fig. 9.

Finally, we calculate the average flow of pedestrians through an exit with arbitrary width  $w \in \mathbb{N}$ . The relation between the width of an exit and the outflow is an important study which has been investigated previously experimentally

[14,15]. When pedestrians move to the exit cell along the shortest path, social morals may prevent pedestrians from breaking into the line. Thus, they do not gather around the exit in disorder, but tend to form lines in front of the exit. Moreover, they do not easily change lanes in a crowd situation. There are also experimental results showing that the pedestrian outflow increases linearly as the width of the exit increases [15]. Therefore, we can represent the average flow through the exit with cell width  $w$  by the linear sum of  $\langle q_1 \rangle$ ,  $\langle q_2 \rangle$ , and  $\langle q_3 \rangle$ . Here we consider two types of exit: an exit at the center of the wall (Ce exit) and an exit at the corner of the room (Co exit). The Ce exit ( $w \geq 2$ ) is divided into  $\langle q_1 \rangle$

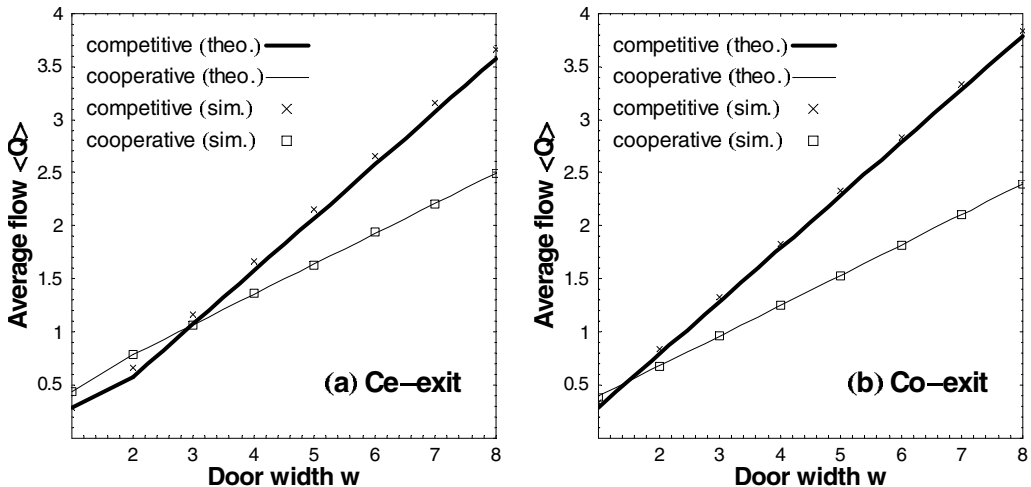


FIG. 13. Average flow for various exit door widths  $w$ . (a) Ce exit. (b) Co exit. We observe the crossing of the two curves in both (a) and (b).

exits and  $\langle q_2 \rangle$  exits, and the average flow through an exit with cell width  $w$ ,  $\langle Q_{\text{center},w} \rangle$ , is described as

$$\langle Q_{\text{center},w} \rangle = \begin{cases} \langle q_3 \rangle & (w=1), \\ 2\langle q_2 \rangle + (w-2)\langle q_1 \rangle & (w \geq 2). \end{cases} \quad (13)$$

In a similar way, the Co exit is divided into  $\langle q_1 \rangle$  exits and  $\langle q_2 \rangle$  exits, and the average flow through an exit with cell width  $w$ ,  $\langle Q_{\text{corner},w} \rangle$ , is described as follows:

$$\langle Q_{\text{corner},w} \rangle = \langle q_2 \rangle + (w-1)\langle q_1 \rangle \quad (w \geq 1). \quad (14)$$

Examples of dividing Ce and Co exits ( $w=3$ ) are shown in Fig. 10. We also define the average flow per one cell as

$$\langle q_{\text{center}} \rangle = \langle Q_{\text{center},w} \rangle / w,$$

$$\langle q_{\text{corner}} \rangle = \langle Q_{\text{corner},w} \rangle / w. \quad (15)$$

## V. COMPARING THE AVERAGE FLOWS FROM ANALYSIS AND SIMULATION

In this section, we compare the analytical and computational results for the average flow  $\langle q \rangle$ , which is a function of  $\beta$ . The parameters of the FFs are set at  $k_s=10$  and  $k_d=0.0$  so that pedestrians move to the exit along the shortest path. The size of the room used in simulation is  $11 \times 11$  cells. The Ce exit room has the exit cells at the centers of the boundary cells of one side of the room, and those of the other sides are all entrance cells where pedestrians come in with the probability 1. Similarly, the Co exit room has the exit cells at the corners of the room, and the boundary cells of two sides that do not include the exit cells are all entrance cells. The examples of the  $5 \times 5$  rooms are shown in Fig. 11. We simulated 11 000 time steps with the initial condition that pedestrians occupy all cells except exit and obstacle cells. Then the average flow of 10 000 time steps from 1001 to 11 000 is used for Fig. 12. It shows average pedestrian flows at the exit as a function of  $\beta$  for various  $\mu$  values. We see that the simulations agree with the analytical results very well. The errors become large for  $\mu=0.9$  since pedestrians conflict with each other and then they cannot move either to the exit cells or to other cells. Surprisingly, for  $\mu=0.9$ , we clearly find that a maximum flow is attained at one value of  $\beta$  in both simulations and analytical results. We call it the optimal  $\beta$ , denoted as  $\beta_{\text{opt}}$  hereafter. For  $\mu \rightarrow 1$  the number of unsolved conflicts increases as  $\beta$  grows. As a result, pedestrians stick and the average pedestrian flow decreases. We also find that the differences between the flows for different  $\mu$  get smaller as  $w$  increases, by comparing the lengths of the arrows in Fig. 12, i.e., the arrow C is shorter than A and D is shorter than B. For the same  $w$  the differences between the flows for different  $\mu$  are smaller at the Co exit than at the Ce exit since the arrow B is shorter than A and D is shorter than C.

## VI. COMPETITIVE AND COOPERATIVE BEHAVIOR AND THE WIDTH OF AN EXIT

Kirchner *et al.* studied how the pedestrians' mood influences the evacuation time [10]. Both the experimental and

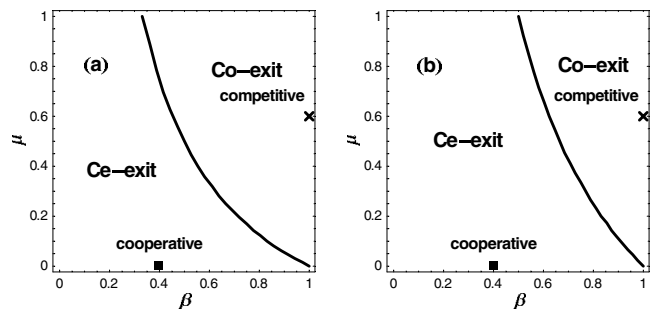


FIG. 14. Curves of  $\beta_c$  on the  $\beta$ - $\mu$  plane. (a)  $w=1$ . (b)  $w \geq 2$ . The flow at the Co exit is larger than the flow at the Ce exit in the upper right region in the figures. In the lower left region, the Ce exit flow is larger.

the computational results show that competition is beneficial if the exit exceeds a certain width, and harmful if the exit width is lower than that. We explain this phenomenon by the analytical solutions (13) and (14). In Ref. [10], competition is described as increased assertiveness (large  $k_s$ ) and a strong hindrance in conflict situations (large  $\mu$ ). Cooperation is represented by small  $k_s$  and vanishing  $\mu$ . In our model, we describe the assertiveness using  $\beta$ . We use  $\mu$  as a parameter of hindrance in conflict situations and its values are the same as in Ref. [10]. The parameters are set at  $\beta=1.0$ ,  $\mu=0.6$  for the competitive situation and  $\beta=0.4$ ,  $\mu=0.0$  for the cooperative situation.

Figure 13 shows the average flows for variable door width  $w$ . The results of analysis agree with those of the simulation very well. The simulation conditions are the same as we described in Sec. V; however, we used  $12 \times 12$  rooms to set up the exit at the center of the boundary cells of the room if the width of the exit is an even number. The size of the room does not influence the average flow since most of the cells are occupied by pedestrians. Clearly, we can observe the crossing of the two curves at a critical door width  $w_c \approx 3$  in Fig. 13(a). Our result corresponds well to the result of Ref. [10], which is  $w_c \approx 2.5$ . This means that we should cooperate with each other to increase the average pedestrian flow when the width of the exit is small. On the contrary, when the width of the exit is large, we do not have to give way to other pedestrians and should go through the exit aggressively. When the exit door is at the corner of the room, the crossing is observed at  $w_c \approx 1.5$  in Fig. 13(b). Therefore, the Co exit is more suitable for a competitive situation than the Ce exit.

The Japanese building standards law [16] gives an average pedestrian flow 1.5 persons/(m s) if an exit is directly connected to the ground. We find that this value significantly changes depending on the pedestrians' moods, i.e., competitive or cooperative. From Fig. 13 we obtain the values of the average flow through the Ce exit, i.e., 1.5 persons/(m s) in the competitive situation and 2.0 persons/(m s) in the cooperative situation. The values are calculated by defining the cell size as  $50 \times 50$  cm<sup>2</sup> and using a pedestrian velocity of 1.3 m/s, which is according to the Japanese building standards law.

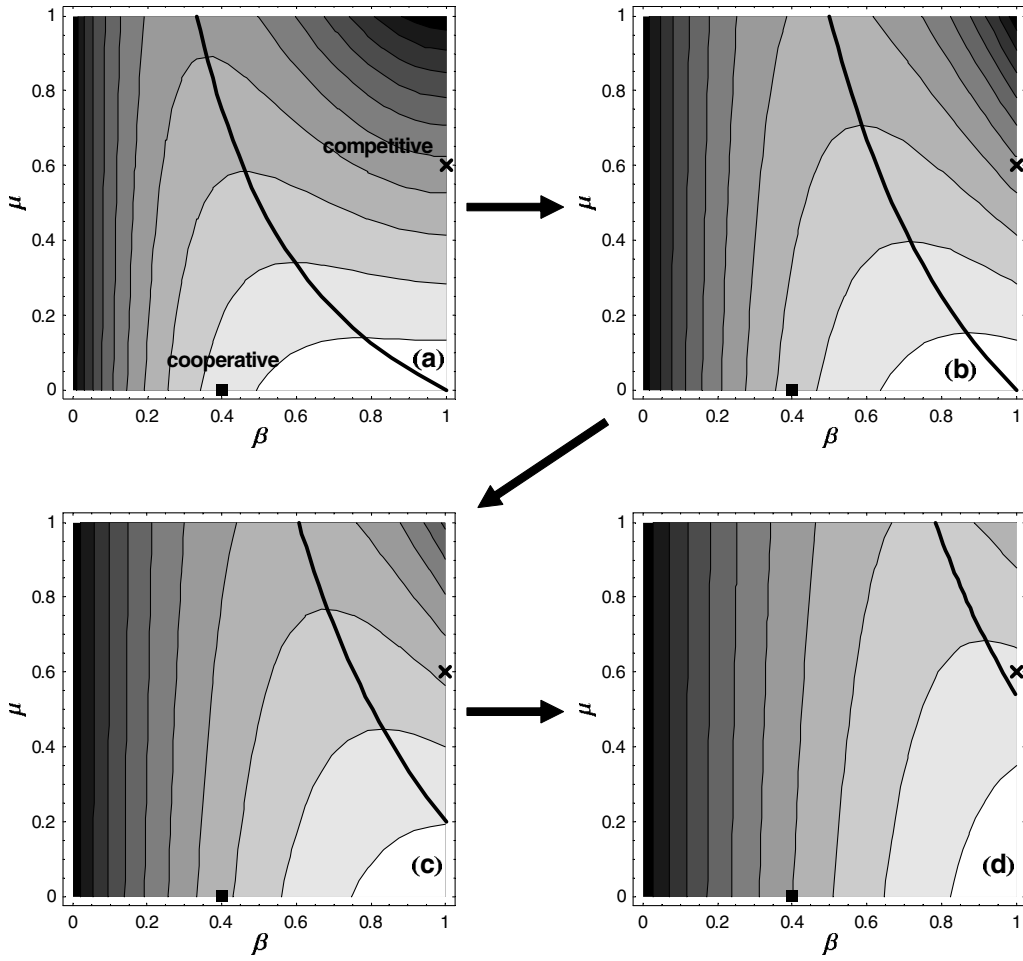


FIG. 15. Contours of average flows for various widths of the exit and its position. (a) Ce exit,  $w=1$ . (b) Co exit,  $w=1$ . (c) Ce exit,  $w=3$ . (d) Co exit,  $w=3$ . ■ represents the competitive situation and ✕ represents the cooperative situation given in Sec. VI. Black bold curves represent  $\beta_{\text{opt}}$ , which moves to the right in the order (a), (b), (c), and (d). In (a) and (b) flow in the cooperative situation is larger than that in the competitive situation. In (c) the average flows are almost the same in both the competitive and the cooperative situations. In (d) flow in the competitive situation is larger. These figures show that flow in the competitive situation gets larger than that in the cooperative situation on increasing the width of the exit and also because of the effect of a wall.

## VII. COMPETITIVE AND COOPERATIVE BEHAVIOR AND THE EFFECT OF A WALL

Here we compare the average flows of Ce and Co exits, and discuss how a wall has an effect on them. The difference between  $\langle Q_{\text{center},w} \rangle$  and  $\langle Q_{\text{corner},w} \rangle$  is calculated as follows:

$$\begin{aligned} & \langle Q_{\text{corner},w} \rangle - \langle Q_{\text{center},w} \rangle \\ &= \begin{cases} -\beta \left( \beta - \frac{1}{1+2\mu} \right) (\beta-1)A & (w=1), \\ \beta \left( \beta - \frac{1}{1+\mu} \right) B & (w \geq 2), \end{cases} \quad (16) \end{aligned}$$

where  $A$  and  $B$  are positive in the entire domain of  $\beta$  and  $\mu$  and are described by

$$\begin{aligned} A &= \frac{\alpha^2(1+2\mu)}{[\alpha+2\beta-(1+\mu)\beta^2]} \\ &\times \frac{1}{[\alpha+3\beta-3(1+\mu)\beta^2+(1+2\mu)\beta^3]}, \end{aligned}$$

$$B = \frac{\alpha^2(1+\mu)}{(\alpha+\beta)[\alpha+2\beta-(1+\mu)\beta^2]}. \quad (17)$$

We obtain  $\beta_c$ , which is the value of  $\beta$  where  $\langle Q_{\text{center},w} \rangle$  equals  $\langle Q_{\text{corner},w} \rangle$ , as follows:

$$\beta_c = \begin{cases} \frac{1}{1+2\mu} & (w=1), \\ \frac{1}{1+\mu} & (w \geq 2). \end{cases} \quad (18)$$

The curves of (18) are drawn in Fig. 14. They divide the  $\beta$ - $\mu$  plane into two regions. In the lower left region, the Ce exit flow is larger and in the upper right region the Co exit flow is larger. We also plot the competitive and cooperative situations used in Sec. VI. The figures show that the Co exit flow is larger in the competitive situation since the wall prevents pedestrians from rushing to the exit at the same time, but the Ce exit flow is larger in the cooperative situation. From this result, we can say that an exit should be at the center of a

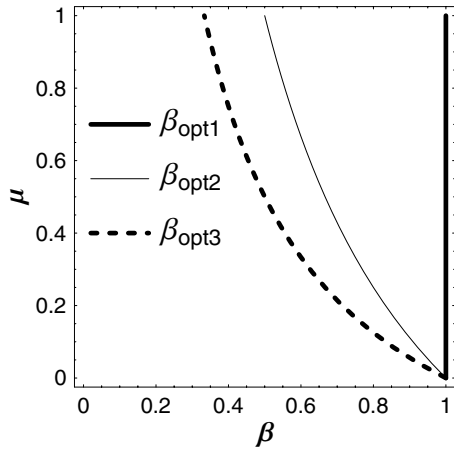


FIG. 16. Curves of  $\beta_{\text{opt}1}$ ,  $\beta_{\text{opt}2}$ , and  $\beta_{\text{opt}3}$ . We see that the curve of  $\beta_{\text{opt}3}$  is the furthest left, that of  $\beta_{\text{opt}2}$  is in the middle, and that of  $\beta_{\text{opt}1}$  is the furthest right.

wall when pedestrians are in a cooperative mood, and at the corner of the room when people are in a competitive mood.

### VIII. CHANGE OF CONTOUR PLOTS OF THE AVERAGE FLOW

The average pedestrian flow through an exit is decided by three parameters:  $\alpha$ ,  $\beta$ , and  $\mu$  according to (10). Since we have set  $\alpha=1$  in this paper, the average flow is determined by  $\beta$  and  $\mu$ . Figure 15 shows contour plots of the average flow, in terms of  $\beta$  and  $\mu$ . Figures 15(a)–15(d) correspond to Figs. 12(a)–12(d), respectively. The flow is large in the white region and small in the black region. The values of the flow are normalized in each figure to draw the gray scale figures. The thick curves in the figures are the curves of  $\beta_{\text{opt}}$ , which gives the maximum average flow in the case of a constant  $\mu$ .  $\beta_{\text{opt}}$  curves divide the plane into two regions. In the upper right regions, pedestrians should slow down further to avoid a conflict, and in the lower left regions, they have to speed up to increase the average flow around the exit. We calculate  $\beta_{\text{opt}1}$ ,  $\beta_{\text{opt}2}$ , and  $\beta_{\text{opt}3}$  from  $\langle q_1 \rangle$ ,  $\langle q_2 \rangle$ , and  $\langle q_3 \rangle$  given in (12), respectively, as follows:

$$\begin{aligned}\beta_{\text{opt}1} &= 1, \\ \beta_{\text{opt}2} &= \frac{1}{1+\mu}, \\ \beta_{\text{opt}3} &= \frac{1}{1+2\mu}.\end{aligned}\quad (19)$$

The  $\beta_{\text{opt}}$  expressions for  $\langle Q_{\text{center},w} \rangle$  and  $\langle Q_{\text{corner},w} \rangle$  are straightforward, but not expressed in a simple form, so we omit them in this paper. We also plot the competitive and cooperative situations used in Sec. VI in the figures.

We see that the  $\beta_{\text{opt}}$  curves move to the right in the order (a), (b), (c), and (d). This is explained by (13), (14), and (19). First, we compare the  $\beta_{\text{opt}}$  curve positions of  $\beta_{\text{opt}1}$ ,  $\beta_{\text{opt}2}$ , and  $\beta_{\text{opt}3}$  in the  $\beta$ - $\mu$  plane using (19). The curve of  $\beta_{\text{opt}3}$  is the

furthest left, that of  $\beta_{\text{opt}2}$  is in the middle, and that of  $\beta_{\text{opt}1}$  is the furthest right (Fig. 16). Next, the expressions for the average flow corresponding to (a), (b), (c), and (d) are described as follows:

$$\begin{aligned}Q(a) &\equiv \langle Q_{\text{center}}(w=1) \rangle = \langle q_3 \rangle, \\ Q(b) &\equiv \langle Q_{\text{corner}}(w=1) \rangle = \langle q_2 \rangle, \\ Q(c) &\equiv \langle Q_{\text{center}}(w=3) \rangle = 2\langle q_2 \rangle + \langle q_1 \rangle, \\ Q(d) &\equiv \langle Q_{\text{corner}}(w=3) \rangle = \langle q_2 \rangle + 2\langle q_1 \rangle.\end{aligned}\quad (20)$$

Now we see clearly why the  $\beta_{\text{opt}}$  curve of  $Q(b)$  is further right than that of  $Q(a)$ .  $Q(c)$  includes  $\langle q_2 \rangle + \langle q_1 \rangle$  more than  $Q(b)$ , and  $Q(d)$  includes  $2\langle q_1 \rangle$  more than  $Q(b)$ . Therefore, the  $\beta_{\text{opt}}$  curve moves to the right in the order (a), (b), (c), and (d).

In the lower left regions of the figures, the average flow increases as  $\beta$  increases, but in the upper right regions, it decreases as  $\beta$  increases for fixed  $\mu$ . Thus the flow-increasing region expands as the  $\beta_{\text{opt}}$  curves move to the right. This makes an exit more suitable to the competitive situation than the cooperative situation. We can see that increase of the width of the exit and the effect of a wall make the average flow larger in a competitive than in a cooperative situation, since the  $\beta_{\text{opt}}$  curves move to the right both on increasing the width of the exit [(a),(b) vs (c),(d)] and by the effect of a wall [(a),(c) vs (b),(d)].

### IX. CONCLUSION

We have introduced into the FF model the effect of slowing down of pedestrians around an exit, and obtained an analytical expression for the average flow through an exit with arbitrary width  $w$  cells by employing the cluster approximation. It turns out that the theoretical results agree quite well with the simulations. The effects of pedestrian mood, the width of the exit, and the wall effect are also studied. The critical exit door width, which was obtained experimentally and was reproduced by simulations in Ref. [10], is also analytically obtained in this paper. We find that an exit should be at the center of a wall in a cooperative situation, whereas it should be at the corner of the room in the competitive situation for a smooth evacuation. The theoretical results also tell us that the unsolved conflicts between pedestrians around the exit are the main cause of decrease in the average pedestrian flow. Therefore, we should consider how to decrease conflicts at a bottleneck to get large pedestrian outflow.

It is important to study pedestrian behavior quantitatively by theoretical analysis, since its dynamics are mainly studied by simulations so far. The Japanese building standards law gives the average pedestrian flow through an exit as a constant value 1.5 persons ( $\text{m s}$ )[16]. Our expression for the average pedestrian flow is more precise and realistic; thus our results can be applied to the design of buildings so that pedestrians evacuate safely and quickly. For example, many present concert halls have an exit at the center of a wall;

however, according to our study we can shorten the evacuation time by setting up an exit at the corner of the hall when people rush to the exit in a competitive mood.

In this paper, we consider the average flow through the exit with more than one cell as the linear sum of the flows through an exit with one cell. In a calm situation, social morals prevent pedestrians from cutting into lines; however, in a panic situation, the pedestrians break into lines to save

their lives. Introducing such interactions between neighboring cells of an exit in detail is the subject of future work.

## ACKNOWLEDGMENTS

We thank Andreas Schadschneider, Armin Seyfried, and Christian Rögsch for useful discussions.

- [1] D. Helbing and P. Molnar, Phys. Rev. E **51**, 4282 (1995).
- [2] D. Helbing, I. Farkas, and T. Vicsek, Nature (London) **407**, 487 (2000).
- [3] D. Helbing, Rev. Mod. Phys. **73**, 1067 (2001).
- [4] C. Burstedde, K. Klauck, A. Schadschneider, and J. Zittartz, Physica A **295**, 507 (2001).
- [5] D. Yanagisawa and K. Nishinari, in Proceedings of the 11th Symposium on Simulation of Traffic Flow, edited by Y. Sugiyama, (Nagoya University, 2005) p. 41 (in Japanese).
- [6] W. Song, X. Xu, B. Wang, and S. Ni, Physica A **363**, 492 (2006).
- [7] R. Jiang and Q. S. Wu, Physica A **364**, 457 (2006).
- [8] W. G. Weng, T. Chen, H. Y. Yuan, and W. C. Fan, Phys. Rev. E **74**, 036102 (2006).
- [9] A. Kirchner and A. Schadschneider, Physica A **312**, 260 (2002).
- [10] A. Kirchner, H. Klupfel, K. Nishinari, A. Schadschneider, and M. Schreckenberg, Physica A **324**, 689 (2003).
- [11] A. Kirchner, K. Nishinari, and A. Schadschneider, Phys. Rev. E **67**, 056122 (2003).
- [12] K. Nishinari, A. Kirchner, A. Namazi, and A. Schadschneider, IEICE Trans. Inf. Syst. **E87-D**, 726 (2004).
- [13] C. M. Henein and T. White, Physica A **373**, 694 (2007).
- [14] Tobias Kretz, Anna Grünebohm, and Michael Schreckenberg, J. Stat. Mech.: Theory Exp. (2006) P10014.
- [15] Armin Seyfried, Tobias Ruprecht, Oliver Passon, Bernhard Steffen, Wolfram Klingsch, and Maik Boltes, e-print arXiv:physics/0702004.
- [16] *The Explanation and Examples of Calculation of Testing the Safeness of Evacuation 2001*, edited by Ministry of Land, Infrastructure and Transport et al. (INOUE SHOIN, 2001), pp. 303–304 (in Japanese).